MRI by steering resonance through space

Angela Lynn Styczynski Snyder[1], Curtis A Corum[1], Steen Moeller[1], Nathaniel J Powell[2], and Michael Garwood[1]

[1]*Department of Radiology, University of Minnesota, Minneapolis, MN, United States,* [2]*Department of Neuroscience, University of Minnesota, Minneapolis, MN, United States*

INTRODUCTION: MRI using spatiotemporal-encoding has been implemented in several forms and demonstrated notable advantages over classic frequency and phase encoding in particular applications and especially for compensating for B_0 and B_1 inhomogeneity (1-6). These previous implementations use a time-dependent pulse frequency $\omega_{RF}(t)$ and the spatial-temporal encoding occurs in the direction of the gradient G which is not modulated in concert with the RF pulse(s). Described here is a new approach for entirely spatiotemporal image acquisition with two types of frequency sweep, $\omega_{RF}(t)$ and $G(t)$, during excitation. This new MRI method, called STEREO, is based on steering resonance through space in a temporally dependent manner. With this new sequence, in principle, B_0 and B_1 inhomogeneity compensation can be done for each region in space, thereby offering the possibility to better address the inhomogeneity. Here, the feasibility of this new method is demonstrated by *in vivo* imaging of human brain.

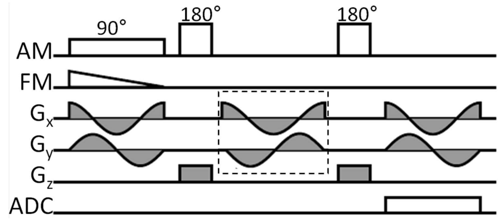

Figure 1 – STEREO implemented as a double SE. A chirp pulse is used for excitation in the presence of a modulated gradient. Signal is refocused and then acquired. TE is constant across the image. The gradient shapes within the dashed box are optional, but can be used to balance asymmetries in the gradient ramps.

THEORY: To achieve time- and space-dependent refocusing in STEREO (Fig. 1), transverse magnetization is excited along a spiral-shaped trajectory in space and time, and subsequently measured in a "pseudo" echo created by two slice-selective 180° pulses. The profile of this spiral-shaped region of resonance is governed by two degrees of signal localization: the RF frequency sweep provides one degree of localization, which is equivalent to the time encoding dimension of other spatiotemporal sequences, and the other degree of localization is imparted by the simultaneous dynamic gradients. Rotated gradients cause the angular position of the excitation to move accordingly. As such, excitation is both rotating and translating from the largest offset-frequency toward zero frequency-offset. A 2D Bloch-based simulation of STEREO (Fig. 2a) shows the simulated magnitude of the transverse magnetization at a singular time point during the excitation, confirming that the greatest excitation is along the trajectory, but also that the excitation is not limited to a single point but rather a region of resonance. Figure 2b shows the maximum magnitude of the transverse magnetization. While the maximum signal is well localized to the trajectory, because the acquired signal is a summation over the spatial domain, the contributions from other regions, while proportionally much weaker than the signal from the trajectory, constitute a substantial part of the total signal, suggesting that an inverse problem reconstruction is well suited to reconstruct the image.

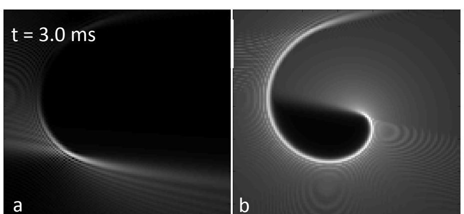

Figure 2 – These simulated profiles show the magnitude of the transverse magnetization in space at one point in time (a) and the maximum of each point from the duration of the excitation (b).

METHODS: A 4 T magnet having a 90 cm bore diameter (Oxford) was used with a clinical gradient system (Sonata, Siemens) and an imaging spectrometer console (Varian/Agilent). STEREO results were collected with a double-echo sequence using adiabatic 180° pulses. The number of complex points along the trajectory was 512, and the number of rotated spirals collected was 128. Healthy volunteers were studied under a protocol approved by our institution's IRB. The RF coil is a 16-element TEM head coil. STEREO images were collected in the transverse plane with b_w = 40 kHz, s_w = 80 kHz, $T_p = N_p / s_w$ = 6.4 ms, TE = 21 ms, and TR = 4 s. The scout images are GRE images with $T_p = N_p / s_w$ = 6.4 ms, TE = 21 ms, and TR = 4 s. The field of view has a diameter of 30 cm. For reconstruction, the aforementioned Bloch simulation was used to approximate the forward problem, and a truncated singular value decomposition solution was computed (7). Because the known values (128 spirals of 512 points each) greatly exceed the unknown values (51 x 51 pixel image), the problem is heavily over-determined, and the matrix is well conditioned.

RESULTS: Figure 3 shows a brain image obtained with STEREO (Fig. 3b) and a GRE image (Fig. 3a) at the same slice position for comparison. The STEREO image shows some signal dropout which may be related to field inhomogeneity because compensation has not yet been implemented. Both are shown with the same low resolution (51 x 51) for fairness of comparison.

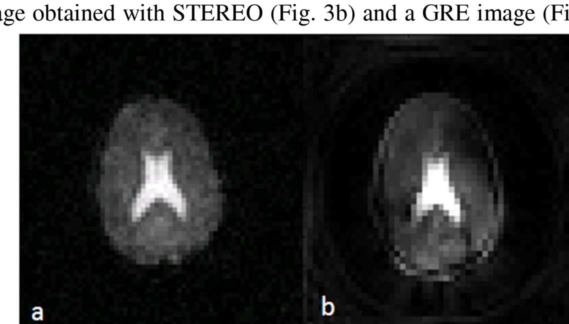

Figure 3 – Comparison of a GRE scout (a) and STEREO (b).

DISCUSSION: STEREO is a new approach to spatiotemporal-encoded MRI, with unique features. Specifically, at any given moment during the pulse, spins are brought into resonance in a limited 2D region in space following a spiral trajectory. This is different from other spatiotemporal encoding techniques which excite planes sequentially in time along a constant gradient direction. In future work, this unique property of STEREO can be exploited to independently adjust for variations in B_0 and B_1 as the excitation trajectory is traced out in space. For example, the RF voltage can be increased when traveling through regions with low B_1. This capability is expected to be advantageous for ultra-high field MRI in which increased field inhomogeneity is particularly problematic. Additionally the ability to image in an inhomogeneous field could help reduce the cost of MRI magnets operating at any field strength.

REFERENCES 1) Meyerand & Wong. MRM 1995. 2) Pipe. MRM 1996. 3) Shrot & Frydman. JMR 2005. 4) Tal & Frydman, JMR 2006. 4) Chamberlain et al. MRM 2007. 5) Ben-Eliezer et al. MRI 2010. 6) Shen & Xiang JMR 2010 7) Hansen. Regularization Tools. 4.1. 2008.

We gratefully acknowledge support from NIH P41 RR008079, S10 RR023730, and S10 RR027290.